Effect of temperature on the development of C-S-H during early hydration of C3S

Maciej Zacak, Sandrine Garrault, J.P. Korb, André Nonat

Effect of temperature on the development of C-S-H during early hydration of C_3S

M. Zajac[1], S.Garrault[1], J-P Korb[2] and A. Nonat[1]
[1]*CNRS-Université de Bourgogne, Dijon, France;* [2]*Ecole Polytechnique, Palaiseau, France*

It is known that accelerating or retarding hydration of OPC by temperature has consequences on the final properties of concrete, the lower the temperature the higher the final compressive strength. It seems that this effect is related to the properties of the hydration layer formed at early age. Early hydration of C_3S has then been studied at temperature ranging from 5 to 45°C in isothermal conditions. The percentage of hydration is estimated from calorimetric measurements and the surface developed by the growth of C-S-H is estimated from Nuclear Magnetic Relaxation Dispersion method. Both data are numerically simulated according to a C-S-H growth model described previously. The good agreement between the experimental and numerical data validates the C-S-H growth model on the tricalcium silicate surface. The higher the temperature, the denser the C-S-H layer is.

1. Introduction

The effect of curing temperature on the strength development is well documented [1-4]: a low temperature of hydration increases the final strength of concrete (at least at 28 days) comparatively to a high temperature when, of course, the strength development at early age is slower. Some investigations reporting the evolution of the percentage of hydration simultaneously to the strength evolution clearly show that it is mainly linked to the kinetics of hydration of silicate phases even if a specific effect of temperature on the strength also exists. The aim of this work is to clarify the effect of temperature on the kinetics of alite hydration at early age and its consequences on the long term evolution. Indeed, it has been clearly shown in previous studies of tricalcium silicate hydration that the conditions of hydration at early age, i.e. especially calcium hydroxide concentration in hydrating solution, considerably influence the process of growth of C-S-H onto the surface of C_3S [5-8] and consequently the properties of the continuous C-S-H layer at the end of the accelerated period of hydration which controls the diffusion limited period.
In the following, we verify in a first section, that the same behavior is observed with tricalcium silicate pastes than the one of cement mortar and

cement concrete. The second part of the paper relates to the study of early hydration temperature on the C-S-H development and its consequences on long term kinetics.

2. Experimental

The experiments have been carried out at three different temperatures: 5, 25 and 45 °C. Between one and ninety days, hydration degree and mechanical properties were monitored by termogravimetric tests (TGA) to determine the amount of nonevaporable water [9-11] and compressive strength measurements using a semiautomatic pneumatic press built in the lab, respectively.

2.1 long term studies

C_3S was mixed with water by hand at laboratory temperature for 120s (C_3S/water = 0.4). The samples were cast into plastic moulds, which form micro cylinders samples (6 mm diameter and 11 mm height), and consolidated by vibration. Moulds were placed in sealed bags and cured at the chosen temperature during one day (two at 5°C) and then demoulded. They were then cured in saturated lime water at the chosen temperature. The hydration of the samples was not stopped before TGA tests that were performed immediately after compressive tests. TGA curves were obtained using a Setaram TG DSC 111 device. Samples (ca 90 mg) were heated at 10°C/min. in the flow of nitrogen (10 mL/min.). The amount of nonevaporable water was defined as:

$$(M_{150} - M_{800})/M_{CEM}$$

where M_{150} and M_{800} are the mass loss of the sample at 150 and 800°C respectively, M_{CEM} is the mass of the C_3S in the sample.

2.2 early age studies

During the first day of hydration (two at 5°C), hydration degree was monitored by isothermal calorimetry. In addition the surface area (Sp_{NMR}) developed by C-S-H during hydration was directly probed by measuring the variation of the spin-lattice relaxation rate R_1 (s^{-1}) = $1/T_1$ of water confined within the hydrated cement with the magnetic field or Nuclear Magnetic Relaxation Dispersion (NMRD). Compared to the other previous NMR methods operating at a fixed and high frequency [12], the benefit of exploring the very low-frequency range is to isolate the typical NMRD dispersion features of the surface contribution of R_1 associated with different processes of molecular surface dynamics [13, 14]. Here we can neglect the bulk and the nuclear paramagnetic contributions always present at high frequency in comparison to the surface diffusion

contribution at proximity of paramagnetic ions (Fe^{3+}) at the C-S-H surface and in exchange with the water of the pore solution [13, 14].This allows us to probe directly the dynamics of proton species at the surface of C-S-H and the specific surface area Sp_{NMR} of these cementitious materials. Moreover, we have recently enlarged the potential use of NMRD to much longer cure times by focusing the measurements of $1/T_1$ only at the lowest possible frequency 10 kHz where we probe only the cross-relaxation of the liquid water specifically with the solid C-S-H hydrates [15].

Calorimetric tests have been done using a TAM Air Isothermal Calorimeter (Thermometrics). 1 gram of C_3S was mixed by hand directly in the calorimetric ampoule with the appropriate amount of water. C_3S and water were previously equilibrated at the experiment temperature.

NMRD measurements were performed on a Stelar Fast Field-Cycling relaxometer (Stelar s.r.l., Mede, Italy) at 10 kHz. 4 grams of C_3S were mixed by hand in a plastic box with the appropriate amount of water using a plastic spatula. C_3S and water were previously equilibrated at the temperature of the experiment. A part of the sample was introduced in a glass tube (6mm in diameter) which was introduced in the relaxometer less than 3 minutes after the beginning of mixing.

2.3 material

The C_3S used in this study was specially synthesized by CTG Italcementi from SiO_2 Aerosil 380 (Degussa), $CaCO_3$ (Prolabo), with a small amount of Fe_2O_3 to introduce paramagnetic impurities for the purpose of NMRD measurements. The chemical analysis of the product determined by X-ray fluorescence is given in **Erreur ! Source du renvoi introuvable.**.

Table 1 : chemical analysis of C3S determined by X-ray fluorescence

SiO_2	25.33 %
Al_2O_3	0.50 %
Fe_2O_3	0.77 %
CaO	73.08 %
MgO	0.08 %

3. Results and discussion

3.1 long term hydration

The evolution of compressive strength and mass loss of the samples cured continuously at 5, 25 and 45 ℃ are plotted o n **Erreur ! Source du**

renvoi introuvable. and **Erreur ! Source du renvoi introuvable.** respectively. As expected, the C_3S paste subjected to the highest

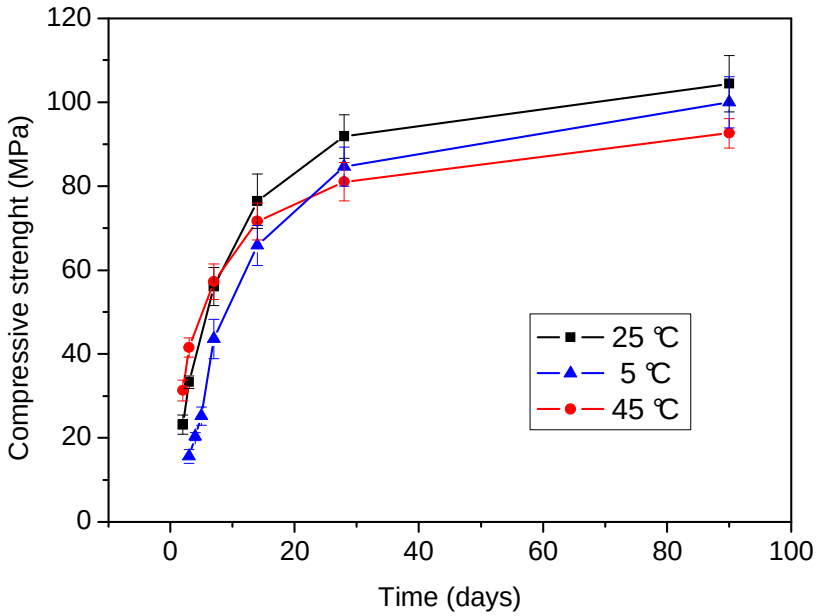

Figure 1 : Evolution of the compressive strength versus time of curing of C_3S pastes hydrated at 5, 25 and 45℃ respectively. E ach point is the average of measurements on at least 10 samples. The error bars are twice of the standard deviation.

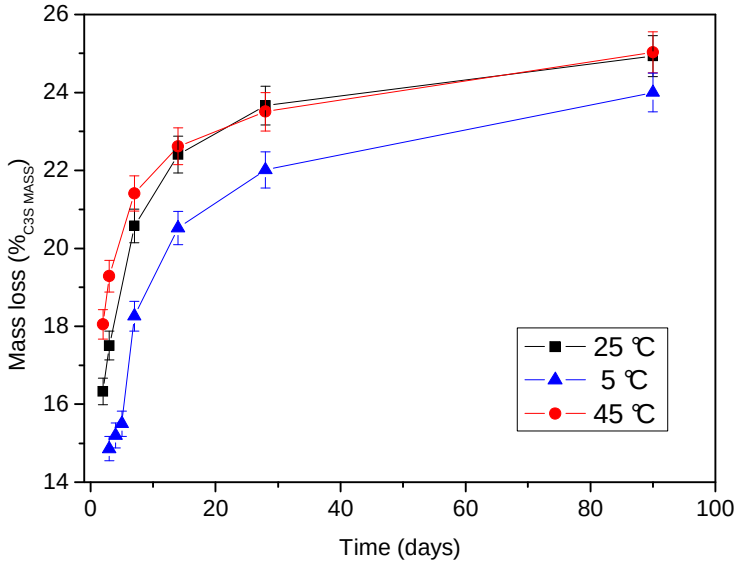

Figure 2: Evolution of the percentage of non evaporable water versus time of curing of C_3S pastes hydrated at 5, 25 and 45℃ respectively. E ach

point is the average of measurements on at least 8 samples. The error bars are twice of the standard deviation.
temperature attains greater early age strength, but finally attains a lower later age compressive strength, whereas the paste subjected to a low temperature leads to lower early-age strength however gets the highest compressive strength after 90 days of hydration (**Erreur ! Source du renvoi introuvable.**). In accordance with compressive strength evolution, the highest hydration degree at early age is achieved for the samples hydrated at the highest temperature; however, with increasing time of curing, the hydration rate is smaller for the highest curing temperature and, after 90 days, differences between the advancement of hydration are similar to the errors bars (**Erreur ! Source du renvoi introuvable.**).

Plotting the evolution of the compressive strength of the sample versus their mass loss representative of their percentage of hydration (**Erreur ! Source du renvoi introuvable.**) gives similar features than those observed for cement mortars and concretes [16]. We observe three parallel lines shifted according to the increase of the curing temperature: the samples cured at different temperatures, have different resistances despite of the degree of hydration is the same. Nevertheless, for a given increase of the amount of the hydration products, the same increase of compressive strength was found. That means that product of hydration formed after one or two days of hydration contributes in a same way to the mechanical properties of the paste and the origin of the differences is due to the product formed at the beginning of hydration.

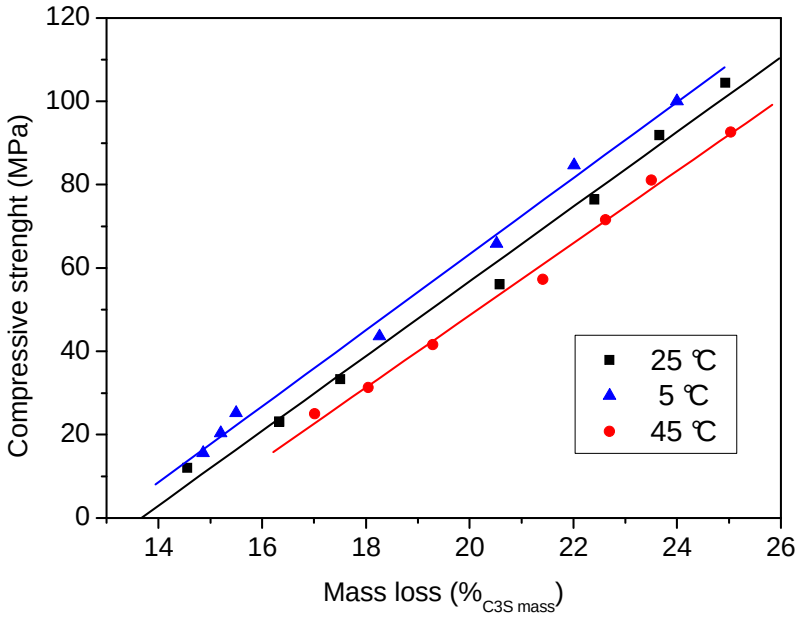

Figure 3 : Evolution of the compressive strength of C_3S pastes versus their percentage of non evaporable water in the case of samples cured at 5, 25 and 45°C respectively.

3.2 early age hydration

The advancement of hydration of C_3S pastes at the three studied temperatures has been estimated from the total heat liberated by hydration at each time. It is obtained by integrating the heat evolution rate curves recorded by isothermal calorimetry and according to

$$\alpha(t)_{C3S} = \frac{Q(t)_{C3S}}{\Delta H_{C3S}} \cdot 100\%$$

The reaction enthalpies at different temperatures were calculated like in [17] (**Erreur ! Source du renvoi introuvable.**).

Table 2 : Enthalpies variation for reaction
$5C_3S + 12H_2O \rightarrow C_8S_5H_{10} + 7CH_2$ at different temperatures.

T (K)	ΔH (kJ mol^{-1})	ΔH (J g^{-1})
313.15	107.45	470.60
303.15	106.26	465.68
298.15	105.07	460.16
293.15	104.47	457.54
288.15	103.87	254.93
278.15	102.68	449.70

The results are plotted on **Erreur ! Source du renvoi introuvable.**. As expected, hydration accelerates very early at 45°C, the rate is very high due to Arrhenius effect and the reaction becomes limited by diffusion very early (near 500 minutes). On the contrary, at the lowest temperature, hydration acceleration occurs only after 1000 minutes, the rate remains relatively slow and the diffusion limited process does not occur before 4000 minutes. The diffusion limited process occurs when the C_3S surface is completely covered by C-S-H.

It is now generally agreed that the development of C-S-H on the surface of C_3S follows a nucleation growth process. It has been described as an anisotropic aggregation of C-S-H nanoparticles around nuclei dispersed on the surface with two different growth rates, respectively parallel and perpendicular to the surface of the C_3S grains [7, 8]. Numerical

simulations of this process account for well with experimental data. The inflexion point on the advancement curve i.e. the maximum of the growth rate corresponds to the moment when the growth sites begin to coalesce. From this time, the rate does not increase anymore because the surface developed by C-S-H stops to increase in the same way. Plotting the

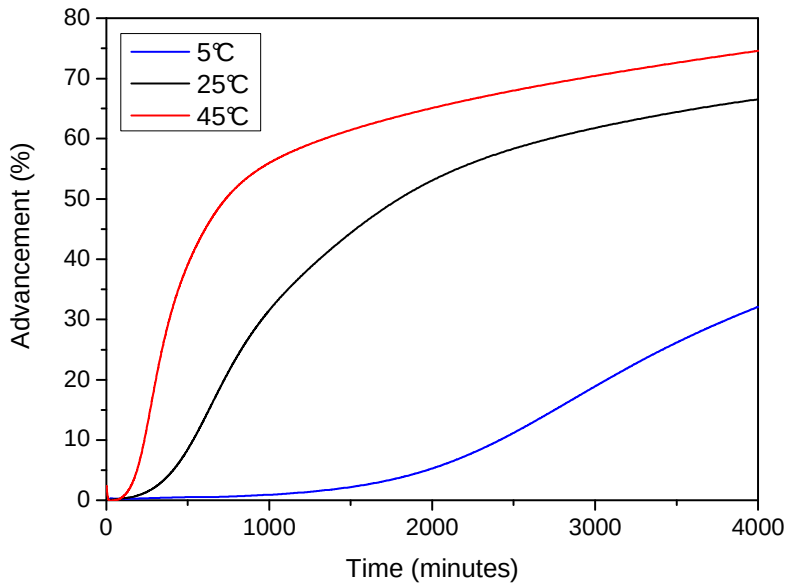

Figure 4 : Evolution of the percentage of hydration versus time of curing of C_3S pastes hydrated at 5, 25 and 45℃ respectively (w/c=0.375).

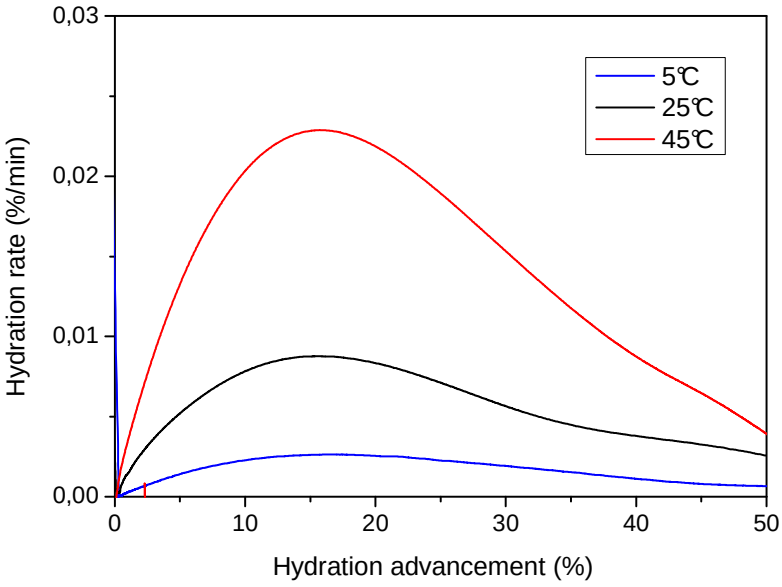

Figure 5 : hydration rate of C_3S in function of the hydration advancement in the case of samples hydrated at 5, 25 and 45℃ respectively (w/c=0.375).

evolution of the rate of hydration versus the percentage of hydration for each hydration temperature (**Erreur ! Source du renvoi introuvable.**) shows that whatever the temperature the surface of C_3S becomes completely covered by the same amount of C-S-H corresponding to about 15% of hydration of C_3S.

In order to precise the properties of C-S-H growing on the surface of C_3S during the accelerated period, NMR proton relaxation experiment have been performed.
The specific surface of the hydrating material is deduced from the evolution of the relaxation rate R_1 (s^{-1}) of water close to paramagnetic impurities (Fe^{3+}) according to the model developed in [13] [14]. When the pores containing the free water in fast exchange with the surface is large enough (~1µm) which is true during the accelerating period, according to Eq. (1), R_1 is proportional to the surface area $S_{p\,NMR}$ with a coefficient depending on the density of paramagnetic impurities on the surface and on the temperature.

$$R_1 = x\varepsilon\rho_{H_2O}S_{p\,NMR}R_{1S}^{surf} \quad (1)$$

where $x\varepsilon$ is the depth of water transiently in interaction with the CSH surface ($1 \leq x \leq 3$ and ε= 0.3 nm is the water molecular size), ρ_{H_2O} is the

density of water and $R_{1S}^{surf} = \frac{\sigma_S \tau_t(T)}{\delta_{IS}^4} \cdot A(\omega,T)$ where σ_S is the surface density of paramagnetic impurities, τ_t is the correlation time of translation of proton-water spin I, δ_{IS} the smallest distance of approach between spin I and S corresponding to paramagnetic Fe^{3+} spins. $A(\omega,T)$ is a dynamical term that comes from the frequency dependence of the probability of reencounters between proton-water and Fe^{3+} ions. In all our previous NMRD measurements in various cementitious materials $A(\omega,T)$ does not depend on frequency below 23 kHz due to the cross relaxation effects [13] [14]. At 10 kHz, it thus results a net simplification of Eq. (1) which becomes:

$$R_1(T) = ab(T)S_{p\,NMR} \quad (2)$$

In Eq. (2), we have formally isolated the specific surface and the temperature contribution that comes from the dipole-dipole correlation time τ_t. To probe only the specific surface area $S_{P\,NMR}$ from Eq. (2) and to compare the values obtained at different temperatures, we have measured the rate of relaxation of protons R_1 on the surface of the same sample of pure C-S-H, *i.e.* with the same value of $S_{p\,NMR}$ but at three different temperatures. This allows us to identify the relative factor $b(T)$ reported in **Erreur ! Source du renvoi introuvable.**. It is thus possible to introduce a temperature correction coefficient given by an equivalent rate of relaxation at 25°C for the experiments at 5 and 45°C.

Table 3 : Temperature dependence of the rate of relaxation of protons on the surface of pure C-S-H

Temperature	R_1 (s^{-1}) measured	Temperature coefficient $b(T)/b(25°C)$
5°C	142.1	1.186
25°C	168.6	1.000
45°C	197.9	0.852

The evolution of the NMR specific surface $S_{p\,NMR}$ developed by the hydrates during the hydration of C_3S pastes at different temperatures is plotted on **Erreur ! Source du renvoi introuvable.**. At the beginning, the rate of increase of surface area of C-S-H in contact with liquid water follows the same picture than the percentage of hydration; it is all the greater as the temperature is high. However, contrary to the degree of hydration, which is relative to the amount of C-S-H formed and which

increases continuously, the extent of the surface of C-S-H in contact with the pore water passes through a maximum value, decreases and then increases again whatever the temperature. The time of occurrence of the surface maximum is, for each curing temperature, the time corresponding to the inflexion point of the percentage of hydration versus time curve i.e. the time for which the rate of hydration reaches is maximum. This result fully agrees with the model of dispersed growth sites of C-S-H cited above according to which the decrease of the growth rate is due to the decrease of the growing surface due to the coalescence of these growing sites. Simulations of the experimental data at different temperatures according to the C-S-H growth model are plotted on Figure 7. Simulations account for the experimental data, hydration degree estimated from calorimetry experiments and specific surface estimated from NMR relaxometry as well, until the hydration becomes limited by diffusion. The minimum of the surface is reached when the surface of C_3S is completely covered, then hydration becomes limited by the diffusion of water and ions through the continuous layer of C-S-H, and the fibrillar outer product forms creating new surfaces in contact with the pore solution. In these simulations, only the number of initial nuclei and the growth rates parallel and perpendicularly to the surface are changed from a temperature to an other.

The extent of the surface of C-S-H at the maximum is the smallest at the highest temperature. It is a result of a difference of the three parameters controlling the growth cited above.

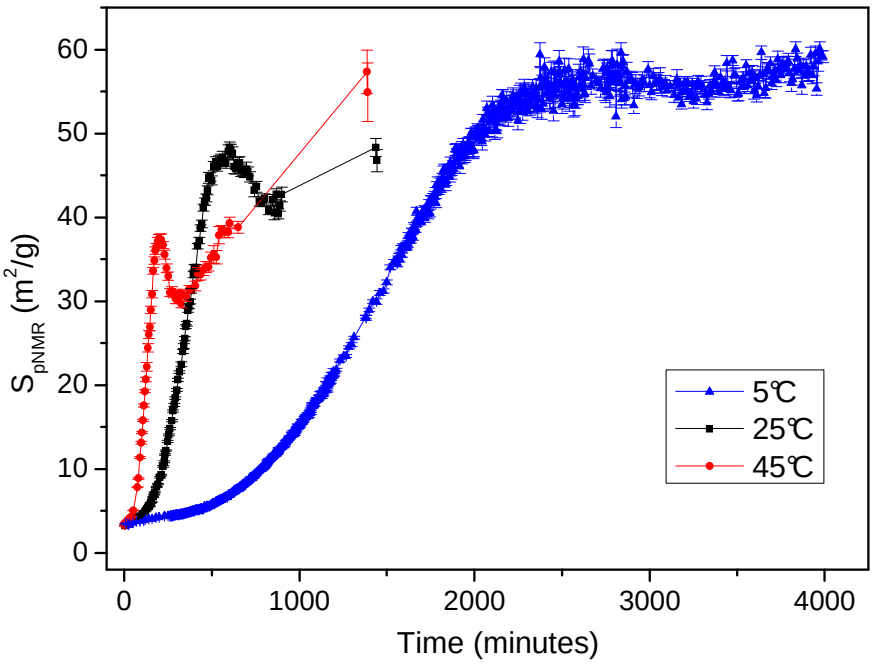

Figure 6 : Evolution versus time of the NMR specific surface area developed in C_3S pastes (w/c=0.375) when they are hydrated at 5, 25 and 45℃, respectively

The evolution of the surface of the hydrates is plotted in function of the percentage of hydration on **Erreur ! Source du renvoi introuvable.**. It clearly shows that, for a same amount of hydrates, the surface developed is all the greater as the temperature is low. In other words, the C-S-H layer formed during the accelerated period is denser at 45℃ than at 25 and 5℃. Consequently, the diffusion of water and ion s through this C-S-H layer is more difficult when it is formed at a higher temperature. That is why the rate of hydration is lower in the diffusion limited period.

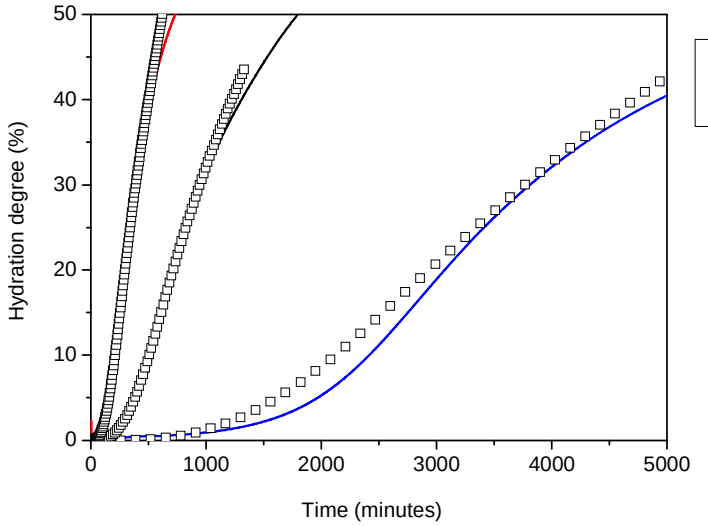

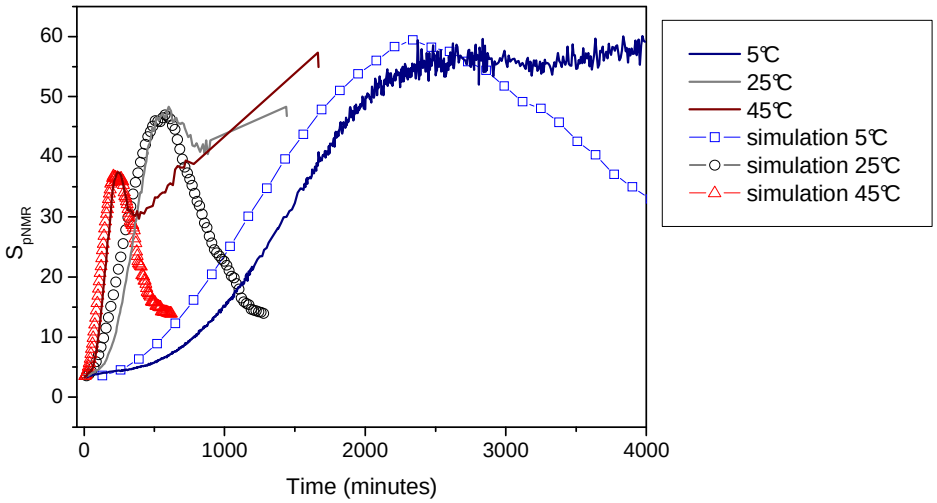

Figure 7 : Numerical simulation of the growth of the C-S-H layer on the surface of C_3S according to the model described in [7]. The parameters of the fits are given in Table 4. The surface developed by C-S-H passes through a maximum like in the NMR experimental data.

4. Conclusion

Probing the amount of C-S-H formed and the surface area developed by the product on the surface of C_3S during the accelerated period of hydration at different temperatures led to show that the properties of the layer are different. The experimental data support the model of formation of the layer by growth around nucleation sites until the coalescence to form a dense continuous layer. The highest the temperature, the denser the layer. This explains the slow rate of hydration of C_3S at high temperature during the diffusion controlled period.

Table 4 : Parameters of the growth model adjusted to fit the percentage of reaction and the surface developed during the hydration of C_3S at different temperatures (advancement factor=0.83, 10-12 % of hydratation/particle, surface factor = 1.6 10^{-7} m^2/g/surface of each face of particle). The dimension of the surface matrix is 2500 x 2500 in all cases (see[7]).

Temperature (℃)	Number of nuclei	parallel growth rate (growth matrix dimension)	Perpendicular growth rate (k)	Scale factor (minute/step)
5	432	9x7	21,6	130
25	300	5x7	11	17,5
45	168	5x7	8,5	5,5

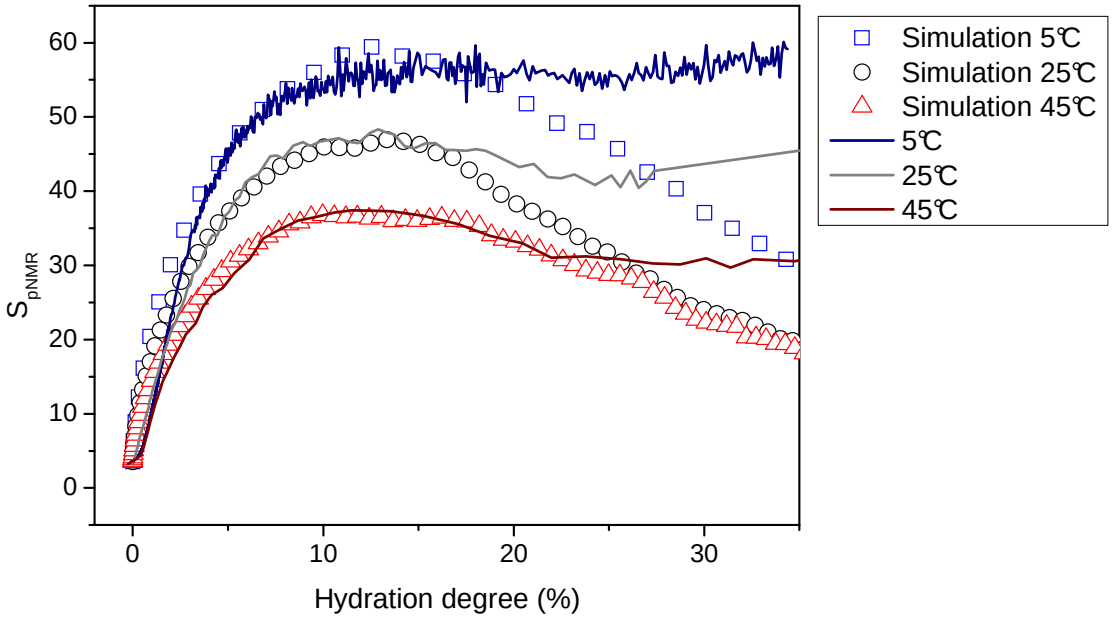

Figure 8 : Evolution of the surface area developed in C_3S pastes (w/c=0.375) deduced from NMRD measurements in function of the hydration advancement in the case of samples hydrated at 5, 25 and 45℃ respectively (w/c=0.375) and simulated results according to the growth model.

5. Acknowledgments

The authors would like to thank ATILH, the French technical association of cement producers, the Région Bourgogne and CNRS for financial support.

6. References

[1] K.O. Kjellsen, R.J. Detwiler, Later-age strength prediction by a modified maturity model. ACI Mater Jour 90 (1993) 220 - 227

[2] J.I. Escalante-Garcia, J.H. Sharp, Effect of temperature on the hydration of the main clinker phases in portland cements part I, neat cements. Cem Conc Res 28(9)(1998) 1245-1257

[3] J.-K. Kim, S.H. Han and Y.C. Song, Effect of temperature and aging on the mechanical properties of concrete: Part I. Experimental results. Cem Conc Res 32(7) (2002) 1087-1094

[4] Kim, J.-K., Moon, Y.-H., and S.-H.Eo, Compressive strength development of concrete with different curing time and temperature. Cem. Conc Res **28**(12) (1998) 1761-1773

[5] D. Damidot and A. Nonat, C_3S hydration in diluted and stirred suspension: (II) properties of C-S-H precipitated during the two kinetic steps. Adv Cem Res **6**(22) (1994) 83-91

[6] A. Nonat, Interactions between chemical evolution (hydration) and physical evolution (setting) in the case of tricalcium silicate, Mater Struct 27(168) (1995) 187-195

[7] S. Garrault and A. Nonat, Hydrated layer formation on tricalcium and dicalcium silicate surfaces : Experimental study and numerical simulations, Langmuir 17(26) (2001) 8131-8138

[8] S.Garrault, T. Behr and A. Nonat, Formation of the C-S-H Layer during Early Hydration of Tricalcium Silicate Grains with Different Sizes, J Phys Chem B, 110(1) (2006) 270-275.

[9] H.F.W. Taylor, Cement Chemistry, Academic Press, New York, 1990

[10] L.J. Parrott, M.Geiker, W.A. Gutteridge and D. Killoh, Monitoring Portland cement hydration: Comparison of methods, Cem Conc Res 20(6) (1990) 919-926

[11] J.I. Escalante-Garcia, Nonevaporable water from neat OPC and replacement materials in composite cements hydrated at different temperatures, Cem Conc Res 33(11) (2003) 1883-1888

[12] M.Letellier, H.Van Damme, B. Mortureux and M.Regourd , Mécanisme d'action des fluidifiants étudiés par RMN du proton. in 8 th. 1986. Rio de Janeiro.

[13] F. Barberon, J.-P. Korb, D. Petit, V.Morin and E. Bermejo, What is the surface specific area of porous cement-based material? A nuclear magnetic relaxation dispersion approach. Magn Reson Imag, 21(3-4) (2003) 355-357

[14] F. Barberon, J.-P. Korb, D. Petit, V. Morin and E.Bermejo, Probing the surface area of cement based materials by nuclear magnetic relaxation dispersion, Phys Rev Lett, 90 (2003) 116103

[15] J.-P. Korb, L. Monteilhet, P.J. McDonald and J. Mitchell, Microstructure and texture of hydrated cement-based materials: A proton field cycling relaxometry approach. Cem Conc Res In press.

[16]K.O. Kjellsen, R.J. Detwiler and O.E. Gjorv, Development of microstructures in plain cement pastes hydrated at different temperatures. Cem Conc Res 21(1) (1991) 179-189

[17] S.A. Grant, G.E Boitnott, C.J. Korhonen and R.S. Sletten, Effect of temperature on hydration kinetics and polymerization of tricalcium silicate in stirred suspensions of CaO-saturated solutions. Cem Conc Res 36(4) (2006) 671-677